

Computer-Aided Molecular Modeling Study on Antibody Recognition of Small Molecules: An Immunoassay for Triazine Herbicides

Meng Yuan,[†] Yu Na,[†] Lingling Li,[†] Bing Liu,[†] Wei Sheng,[†] Xiaonan Lu,^{†,‡} Ivan Kennedy,[§] Angus Crossan,[§] and Shuo Wang^{*,†}

[†]Key Laboratory of Food Nutrition and Safety, Ministry of Education of China, Tianjin University of Science and Technology, Tianjin 300457, China

[‡]School of Molecular Biosciences, College of Veterinary Medicine, Washington State University, Pullman, Washington 99164-7520, United States

[§]Faculty of Agriculture, Food and Natural Resources, University of Sydney, Sydney, New South Wales 2006, Australia

Supporting Information

ABSTRACT: Most immunoassays for determination of small molecules are still designed on the basis of the “trial and error” method, due to the lack of understanding of antibody recognition. In the present study, we developed a heterologous indirect competitive enzyme-linked immunosorbent assay for determination of triazine herbicides, with limits of detection for 11 triazines ranging from 0.05 to 29.4 $\mu\text{g/L}$. Mechanisms of the antigen–antibody interaction were studied by computer-aided molecular modeling (CAMM)-based quantitative structure–activity relationship analyses. Co-effects of the analytes’ substructural hydrophobic, electrostatic, and steric fields on antibody recognition were further revealed. Hydrophobicity of the antigens was demonstrated to have the most important impact. Even less exposed substituents provided hydrophobic force to the antigen–antibody interaction. Dislocated orientation of analyte functional groups could lead to steric hindrance and hydrophobic misleading of antibody recognition. This may happen even when the antigens contained the same substituent as the hapten. Frontier orbital energies also affect the reaction significantly. This study highlights of the power of CAMM-based analyses, providing insights into antibody recognition of small molecules.

KEYWORDS: Triazine, hapten, immunoassays, molecular modeling, antibody recognition

INTRODUCTION

Immunoassay is widely used in clinical, environmental, and food analysis, due to its high accuracy, sensitivity, low cost, and rapidity. To establish sensitive immunoassays, specific antibodies must be available. Small molecules should be coupled to carrier proteins to obtain immunogenicity prior to immunization. Therefore, functional groups should be introduced to haptens to conjugate with proteins.^{1,2} An optimal immunizing hapten for expected analytes has to be a near-perfect mimic of those molecules.³ Most designs of haptens and small-molecular immunoassays are based upon the immunochemists’ experiences and “trial and error” methods, owing to the lack of understanding of the antigen–antibody interaction mechanism.⁴ The empirical design, the introduced spacer arm, and the structural influence by protein may lead to unpredictable structural changes or reduce the rationality of hapten design. Only a few studies have focused on theoretical or molecular-level analyses of the antigen–antibody reaction,^{5,6} relying upon empirical analyses or nonquantitative assessments.

In recent years, computer-aided molecular modeling (CAMM) has been applied to help design haptens rationally, by which specific antibodies have been generated.^{6–8} CAMM-based quantitative structure–activity relationship (QSAR) analyses can explain the cross-reactivities of the established immunoassays.^{4,9–11} However, in these studies, most analyses

were built on the basis of whole molecular structures of analytes, and important features associated with substructures received insufficient attention. For example, contributions of the antigens’ hydrophobicity, one of the most important impact factors in antibody recognition, were not shown due to the limitations of the three-dimensional (3D) QSAR algorithm adopted in these earlier reports.

Triazines are herbicides used worldwide that may remain in ground, water, soil, and many food products, and thus they have become a matter of concern throughout the world.¹² In the present work, a heterologous immunoassay with broad specificity for the detection of triazine herbicides was developed. Furthermore, QSAR methodologies were employed on the basis of experimental data from the developed immunoassay in order to explain the mechanism of triazine–antibody interaction. In brief, a genetic function approximation (GFA) algorithm-based 2D-QSAR model, a Hologram (H-) QSAR model, and a comparative molecular similarity indices analysis (CoMSIA) algorithm-based 3D-QSAR model have been employed to examine the molecular effects. These

Received: July 26, 2012

Revised: October 4, 2012

Accepted: October 8, 2012

Published: October 8, 2012

methodologies can determine specific properties and groups of the analyte molecules that affect the antibody recognition and provide insights into the antigen–antibody interaction.

MATERIALS AND METHODS

Chemicals and Reagents. Triazine standards, bovine serum albumin (BSA), ovalbumin (OVA), complete and incomplete Freund's adjuvant, 3,3',5,5'-tetramethylbenzidine (TMB), and horseradish peroxidase (HRP) were purchased from Sigma–Aldrich (St. Louis, MO). Goat anti-mouse IgG (H+L) HRP conjugate (secondary antibody, 1 mg/mL) was purchased from Promega (Madison, WI). Protein A–Sepharose 4B was from Amersham Biosciences (Uppsala, Sweden).

Carbonate buffer (0.05 M carbonate, pH 9.6) was used for coating antigen onto microtiter plates. Phosphate-buffered saline (PBS) (10 mM phosphate, 137 mM Na⁺, and 2.7 mM K⁺, pH 7.4) was used to dilute immunoreagents and samples. Phosphate-buffered saline with 0.05% Tween 20 (PBST) was applied to wash microtiter plates after each reaction step.

Hapten Design. The common chemical structure of 11 triazines, as well as different substituent groups of haptens 1 and 2 and the 11 triazines labeled as R1, R2, and R3, are shown in Table 1. To provide

Table 1. Substituents of the Triazines

compd	R1	R2	R3
hapten 1	Cl	NH– CH(CH ₃) ₂	NH– (CH ₂) ₃ COOH
hapten 2	S– (CH ₂) ₂ COOH	NH– CH(CH ₃) ₂	NH–CH(CH ₃) ₂
atrazine	Cl	NH– CH(CH ₃) ₂	NH–C ₂ H ₅
propazine	Cl	NH– CH(CH ₃) ₂	NH–CH(CH ₃) ₂
prometryn	S–CH ₃	NH– CH(CH ₃) ₂	NH–CH(CH ₃) ₂
ametryn	S–CH ₃	NH– CH(CH ₃) ₂	NH–C ₂ H ₅
prometon	O–CH ₃	NH– CH(CH ₃) ₂	NH–CH(CH ₃) ₂
terbutylazine	Cl	NH–C(CH ₃) ₃	NH–C ₂ H ₅
simazine	Cl	NH–C ₂ H ₅	NH–C ₂ H ₅
desmetryn	S–CH ₃	NH– CH(CH ₃) ₂	NH–CH ₃
terbumeton	O–CH ₃	NH–C(CH ₃) ₃	NH–C ₂ H ₅
simetryn	S–CH ₃	NH–C ₂ H ₅	NH–C ₂ H ₅
terbutryn	S–CH ₃	NH–C(CH ₃) ₃	NH–C ₂ H ₅

immunogenicity to small molecules, functional groups should be introduced to haptens to couple with carrier proteins. Hapten 1 was designed with a chlorine atom and an isopropylamine group in R1 and R2 positions, respectively, with *N*-butyl acid at R3 position to expose the epitope. For hapten 2, two isopropylamines were exposed with *S*-propyl acid supporting.

Preparation of Haptens and Hapten–Protein Conjugates. The haptens were designed and synthesized in our previous work.¹³ Both haptens were applied to couple with BSA and OVA to prepare the immunogens and coating antigens, respectively. All the conjugates were prepared with the activated *N*-hydroxysuccinimide (NHS) ester method.¹⁴

Production of Polyclonal Antibodies. Both immunogens were used to immunize New Zealand white rabbits (two rabbits for each immunogen) according to the following protocol.¹⁵ Five injections of immunogen at 2-week intervals were given to each New Zealand white

rabbit. For each rabbit, the initial immunizing was performed with the mixture of 1 mg of immunogen and Freund's complete adjuvant (1:1 v/v, 2 mL per rabbit). Then subsequent booster injections were performed with half doses. Ten days after the final boost, the antisera were collected. After purification by protein A–Sepharose 4B affinity chromatography, the IgG fraction was dialyzed and its concentration was 2.6 mg/mL (detected by UV spectrophotometry).

Enzyme-Linked Immunosorbent Assay. Enzyme-linked immunosorbent assay (ELISA) was established on the basis of the common protocol of indirect competitive enzyme-linked immunosorbent assay (icELISA).^{16,17} Coating antigen (100 μL of 1 μg/mL) was coated onto each well in microplates at 4 °C for 16 h. Afterward, 200 μL of 0.5% skim milk powder (diluted with PBS) was used to block each well at 37 °C for 1 h. Then the analytes and optimized dilutions of antibodies dissolved in PBS (40,000-fold diluted for homologous ELISAs and 10,000-fold diluted for heterologous ELISAs), 50 μL/well for each, were simultaneously added and the plates were incubated for 1 h at room temperature, followed by 10,000-fold diluted secondary antibody incubation at 37 °C for 30 min. TMB chromogenic substrate was added to characterize the reaction. After each step, a PBST washing step was carried out. The color development was stopped by adding 50 μL of 2.5 M H₂SO₄, and the absorbance values were read in dual-wavelength mode (450 nm as test wavelength and 650 nm as reference wavelength).

Cross-Reactivities. The icELISA was used to determine the polyclonal antibody (pAb) specificities and cross-reactivities (CRs). For atrazine and propazine, standards were diluted from 40 μg/L. For prometryn, ametryn, prometon, and terbutylazine, standards were diluted from 200 μg/L. For simazine and desmetryn, standards were diluted from 1000 μg/L. For terbumeton, simetryn, and terbutryn, standards were diluted from 5000 μg/L. All standards were 5-fold gradient-diluted. Inhibition ratios, sensitivities (defined as half-maximal inhibition concentration values, IC₅₀), and CRs were calculated as

$$\text{inhibition ratio (\%)} = \frac{A_{\text{control}} - A_{\text{inhibit}}}{A_{\text{control}} - A_{\text{blank}}} \times 100$$

where *A* refers to absorbance, control values were results tested without analytes, and blank values were results without pAb and analytes.)

IC₅₀ value (micrograms per liter) refers to the concentration of analytes that could provide an inhibition ratio of 50%. The cross-reactivity values were calculated according to

$$\text{CR (\%)} = \frac{\text{IC}_{50}(\text{atrazine, } \mu\text{g/L})}{\text{IC}_{50}(\text{analyte, } \mu\text{g/L})} \times 100$$

Quantitative Structure–Activity Relationship Analyses.

Minimum energy conformations of all triazine structures were calculated by use of Hyperchem 8.0 (Hypercube Inc., Gainesville, FL) and Discovery Studio 2.5 (Accelrys Software Inc., San Diego, CA). Briefly, molecular mechanics force field MM+ was used to preoptimize the structures,¹⁸ followed by a AM1 semiempirical quantum chemical optimization¹⁹ to obtain minimum energy conformations.

From the energy-minimized triazine structures, molecular parameters of triazine molecules were calculated, including steric properties [molecular volume, surface area, molecular polar surface area, refractivity, and polar moment of inertia (PMI)], hydrophobic properties [logarithm of octanol/water partition coefficient (log *P*) and molecular solubility], and other physicochemical parameters [molecular weight, number of hydrogen-bond acceptors/donors, number of rotatable bonds, polarizability, dissociation constant (p*K*_a), dipole moment, lowest unoccupied molecular orbital energy (*E*_{LUMO}), highest occupied molecular orbital energy (*E*_{HOMO}), differences between *E*_{LUMO} and *E*_{HOMO} (Δ*E*_{H–L}) (the frontier orbital parameters were calculated in the DMol3 mode)]. In order to understand what and how antigen properties affected the antibody recognition, CAMM-based QSAR calculations were made, and the results were analyzed. Pearson correlation analysis, GFA algorithm-based 2D-QSAR model, HQSAR model, and CoMSIA algorithm-

based 3D-QSAR model analyses have been carried out. Since antigen–antibody reaction is a molar-dependent quantity, molar units were used in the structure–activity relationship studies.⁴ Experimental IC_{50} data in mass units were converted to molar units. pIC_{50} , defined as $-\log IC_{50}$ (in molar units), was used to indicate the activities of antibody recognition.

Pearson Correlation Analysis and Genetic Function Approximation Two-Dimensional Quantitative Structure–Activity Relationship Calculation. Pearson correlation analysis was performed with experimental pIC_{50} data and calculated molecular parameters by use of PASW Statistics 18.0 (SPSS Inc., Chicago, IL). GFA algorithm was applied to build a 2D-QSAR model with the help of Discovery Studio 2.5. The experimental data, pIC_{50} , were used as dependent variables, and calculated molecular parameters were used as independent variables. The calculation protocol was set as follows: linear was chosen as the model form, the equation length was set as 1–4, and all other parameters were kept as default.

Hologram Quantitative Structure–Activity Relationship Calculation. Sybyl-X 1.1 (Tripos Inc., St. Louis, MO) was used to build the HQSAR model. First, the triazine molecular structures were imported to establish a database. After the optimization of hologram lengths, atom count in fragments, and information sources, followed by the set of best model selection protocol (with the least standard error), a spreadsheet was created with the experimental pIC_{50} data. HQSAR was then run to build a model, with which the fragment contributions could be visually investigated.

Comparative Molecular Similarity Indices Analysis Three-Dimensional Quantitative Structure–Activity Relationship Calculation. The CoMSIA model was built with Sybyl-X 1.1. The triazine molecular structures were imported into a database. In conjunction with Gasteiger–Hückel charges, standard Tripos force field with 8 Å cutoff for nonbonded interactions was used to add charges to the molecules, with a 0.005 kcal/(mol·Å) termination gradient, and a dielectric constant of 1.0. The maximum iteration was set as 1000. All molecules were aligned to match the skeleton of the common structure (atoms 1–8, see Figure 1). With a spreadsheet filled with experimental pIC_{50}

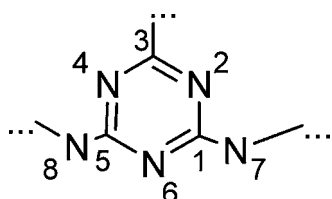


Figure 1. Skeleton of the common structure, with which all molecules were aligned.

values and data calculated with 3-D CoMSIA (steric, electrostatic, and hydrophobic fields) were used, and the attenuation factor was set as 0.3, partial least-squares (PLS) with a leave-one-out (LOO) cross-validation was applied to build the model. The CoMSIA field was used as an independent variable, and the pIC_{50} activity value was used as a dependent variable.

RESULTS AND DISCUSSION

Hapten Design. Two haptens were synthesized (Table 1). For hapten 1, a chlorine atom and an isopropylamine group were exposed in the hapten–protein conjugate. For hapten 2, two isopropylamine groups were exposed in the hapten–protein conjugate.

Haptens 1 and 2 were synthesized and both were applied to prepare immunogens and coating antigens. Antibodies were generated, with which ELISAs for the detection of triazine herbicides were established.

Establishment of Enzyme-Linked Immunosorbent Assays. Four permutations of ELISAs, using both hapten-generated antibodies and coating antigens, were developed.

After the optimization of reaction conditions, the optimal ELISA procedures were obtained. The sensitivities (represented by IC_{50}) of atrazine in the homologous (Ho-) and heterologous (He-) ELISAs are shown in Table 2. The antibody generated by

Table 2. Sensitivities (IC_{50})^a of Atrazine in Homologous and Heterologous ELISAs

type of ELISA	type of hapten		IC_{50} ($\mu\text{g/L}$)
	antibody	coating antigen	
HoELISA 1	hapten 1	hapten 1	18.4
HoELISA 2	hapten 2	hapten 2	29.7
HeELISA 1	hapten 1	hapten 2	1.9
HeELISA 2	hapten 2	hapten 1	2.7

^a IC_{50} , concentration of the analyte that inhibits the maximum signal intensity by 50%.

hapten 1 provided more sensitive recognition for atrazine than the antibody based upon hapten 2. It is widely considered that a proper heterologous competitive antigen could help the immunoassay obtain better sensitivity.²⁰ In the present study, the HeELISAs performed much more sensitively than the HoELISAs. With the best sensitivity to atrazine, HeELISA 1, which employed the antibody generated by hapten 1 and the coating antigen conjugated by hapten 2, was selected for further study.

Immunoassay Sensitivity and Specificity. Eleven triazine structural analogues were applied to evaluate the specificity of the developed ELISA (HeELISA 1). Standard curves are shown in Figure S-1, Supporting Information. The limits of detection (LODs, defined as IC_{15})^{21,22} of the 11 triazines ranged from 0.05 to 29.4 $\mu\text{g/L}$, which were lower than the maximum residue limits (MRLs) for most samples. Thus, this broad-specificity ELISA can be used as an effective tool for monitoring triazine residues.

The IC_{50} values, LODs, and CRs of the triazines based upon the optimal ELISA (HeELISA 1) are listed in Table 3. Atrazine

Table 3. IC_{50} , Limits of Detection, and Cross-Reactivities of Triazines from HeELISA 1

compd	IC_{50} ($\mu\text{g/L}$)	LOD ($\mu\text{g/L}$)	CR (%)
atrazine	1.9	0.15	100.0
propazine	1.6	0.05	119.9
prometryn	10.3	1.4	18.7
ametryn	13.3	2.3	14.5
prometon	13.7	2.6	14.1
terbutylazine	18.1	1.0	10.6
simazine	58.5	4.6	3.3
desmetryn	98.3	12.1	2.0
terbumeton	163.2	10.6	1.2
simetryn	197.9	21.0	1.0
terbutryn	295.8	29.4	0.6

and propazine had the best sensitivities (1.9 and 1.6 $\mu\text{g/L}$, respectively). In addition, the antibody recognition of prometryn, ametryn, and prometon were much lower (IC_{50} = 10.3, 13.3, and 13.7 $\mu\text{g/L}$, respectively), although they have the same R2 and R3 groups as atrazine and propazine. This result indicated that R1 was critical in the antigen–antibody interaction. With less similar functions, other triazines provided variable recognition by the antibody.

However, what properties and how groups affected the antibody–antigen interaction from the quantitative perspective were still not well understood. Therefore, CAMM-based QSAR analyses were performed to provide deeper insights.

Quantitative Structure–Activity Relationship Analyses. QSAR analysis is a computational method by which chemical structure is quantitatively correlated with a biological or chemical reactivity.²³ In recent years, computational molecular modeling and simulation have been applied to obtain the optimal molecular structures, and CAMM-based QSAR analysis has been developed.^{4,9–11} In the present study, advanced algorithms and methods were applied to give a reasonable explanation to the antigen–antibody interaction.

Pearson Correlation Analysis and GFA Algorithm-Based 2D-QSAR Analysis. Pearson correlation analysis was carried out to evaluate the correlations between the experimental data pIC_{50} (defined as $-\log IC_{50}$) and the calculated molecular descriptors. The result of correlation analysis indicated that $\log P$, which represents the hydrophobicities of the compounds, showed the highest correlation with pIC_{50} ($r = 0.748$). As a result, it was assumed that the antigens' hydrophobicity played an important role in antibody recognition. However, other molecular properties including steric or electrostatic effects, which may affect the antibody recognition, were not reflected. Consequently, a 2D-QSAR model was built to evaluate the co-effects of the molecular properties.

GFA models are created by evolving random initial models by use of a genetic algorithm; they offer a new approach to the problem of building QSAR models.²⁴ In the present work, GFA algorithm was used to identify important descriptors so as to build a 2D-QSAR model. The predictive ability of the model was determined by “leave-one-out” (LOO) cross-validation, which involves use of a single observation from the original sample as the validation data and the remaining observations as the training data.²⁵ In the validation method of LOO, the value of statistical characteristic q^2 is considered as a proof of predictive ability of a model. The equation of the QSAR model was concluded as follows:

$$pIC_{50} = -5.74 + 5.61 \log P + 52.0E_{LUMO} + 0.0232PMI$$

where $n = 9$, $R^2 = 0.943$, $q^2 = 0.514$, and $P_F < 0.001$. In this model, ametryn, atrazine, desmetryn, prometryn, propazine, terbutmeton, terbutryn, simetryn, and simazine were chosen as the training set to establish the model. Prometon and terbuthylazine, which could represent different classes of triazine molecules, were chosen as the test set to assess the accuracy and predictive ability (shown in Figure 2, $n = 9$). R^2 higher than 0.9 and P_F lower than 0.001 indicated that this model was significantly correlated with the dependent variable, pIC_{50} . q^2 higher than 0.5 demonstrated that this model had high predictive ability. Further, as shown in Figure 2, since the training spots and the test spots were clustered to the trend line, which had a slope close to 1, it was demonstrated that the model possessed a high correlation and predictive ability. Hydrophobic ($\log P$), electrical (lowest unoccupied molecular orbital energy, E_{LUMO}), and steric (polar moment of inertia, PMI) properties of the analytes co-affected the antibody recognition. It has been reported that frontier-orbital energy may play an important role in antibody recognition.²⁶ In the correlation analysis, E_{LUMO} had high correlation with R1 group (E_{LUMO} had correlations of -0.818 and -0.892 for R1 surface area and $\log P$, respectively). It indicated that R1's ability to accept electrons may affect the antibody recognition. However,

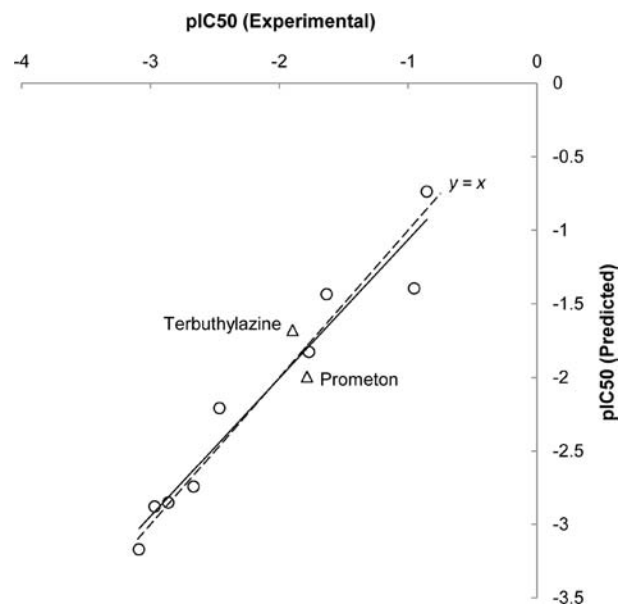


Figure 2. Two-dimensional QSAR model ($n = 9$): experimental vs predicted pIC_{50} values by GFA analysis. Training set (○) and test set (△) were used in this model. The spots were close to the trend line (—) and the $y = x$ line (---), indicating that the model performed with high correlation and predictive ability.

what groups and how substructural properties three-dimensionally affected the antibody recognition was not clear yet. Consequently, HQSAR and CoMSIA analyses were performed to do further studies.

HQSAR Analysis. Molecular Hologram QSAR is a new computer-implemented technique that employs specialized fragment fingerprints (molecular holograms) as predictive variables of biological activity. All possible fragments are color-encoded to show how compounds affect the biological activity.²⁷

To build the HQSAR model, training set and test set were chosen in the same manner as those used to build the 2D-QSAR. The experimental pIC_{50} values were used as the dependent variable. Based upon the optimized parameters of the model (atom count in fragments, 3–5; information sources were atoms, bonds, and hydrogen atoms), an HQSAR model was built showing high correlation ($R^2 = 0.889$) and predictive ability ($q^2_{LOO} = 0.724$). The energy-minimized conformation of hapten 1, as well as the molecular fragments' contribution to pIC_{50} , is shown by color coding (Figure 3). Green and yellow regions represent fragments providing positive contributions to the reaction that increase the antibody recognition. Red and orange contours indicate regions providing negative contributions. White fragments had no or little contribution. All molecules are in their energy-minimized conformations. White color on the hapten does not provide any contributions to the antibody recognition but only provides 3-D structure.

An interesting fact provided by the HQSAR analysis is that although most of the triazines have isopropylamine groups at their R2 position, they had opposite contributions. For atrazine and propazine, which had the highest sensitivities in the ELISA, the isopropylamine groups at R2 contributed positively to antigenicity. On the contrary, the isopropylamine at R2 of ametryn, desmetryn, prometon, and prometryn had negative contributions. It is apparent that positive-contribution-playing isopropylamine groups at R2 (atrazine and propazine) kept

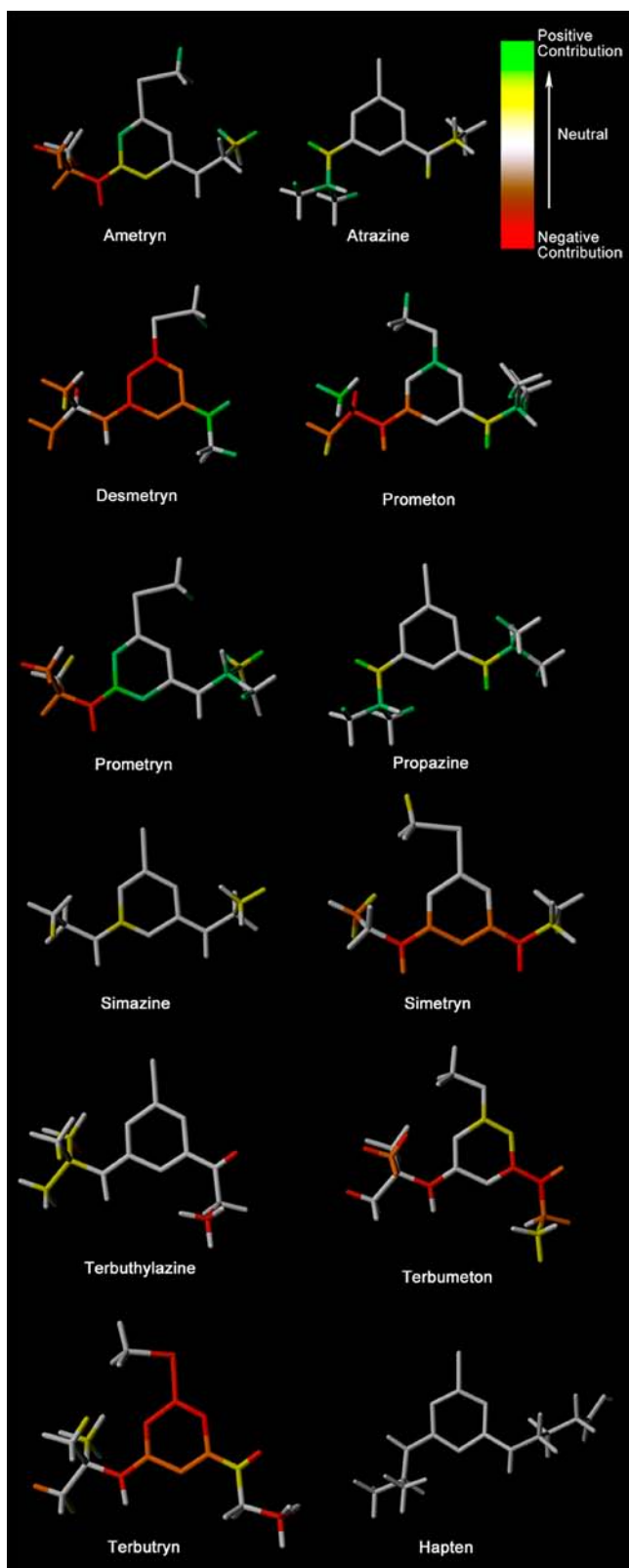


Figure 3. Structural contribution to antibody recognition for triazines based upon HQSAR analysis. Green and yellow regions represent positive contribution; red and orange represent negative contribution.

away from the R1 groups, the same as the structure of the haptin. On the other hand, the isopropylamine groups in the other four triazines approach the R1 groups and create negative contributions. Likewise, although simazine has similar sub-

structures as the haptin, its R2 group approaching R1 decreased the antibody binding and made the sensitivity of simazine far worse than expected. In sum, even though structural analogues have the same function in one position, different functions in other positions could cause steric variations to it and may lead to a totally opposite contribution to the antibody recognition.

The chain in R3 of the haptin was expanded with a direction-relative approach to R1. No matter whether it was isopropylamine or ethylamine, the R3 substituent's approach to R1 contributed positively to the reaction. Conversely, R3 substituents that kept away from R1 played negative roles. Desmetryn was an exception. The R3 away from R1 substituent contributed positively. This is probably because the methylamine at its R3 position was so small that it could be received by the formed R3 pocket even if the group was in a dislocated direction.

It is apparent that, for triazines with the same groups in R1 and R2, more hydrophobic R3 groups provided more hydrophobic contributions according to the HQSAR model. For instance, prometryn with a more hydrophobic R3 group, isopropylamine, showed better recognition ($IC_{50} = 10.3 \mu\text{g/L}$) than ametryn ($IC_{50} = 13.3 \mu\text{g/L}$) with an ethylamine at R3. Desmetryn with a methylamine had even worse sensitivity ($IC_{50} = 98.3 \mu\text{g/L}$). The same situation happened with propazine ($IC_{50} = 1.9 \mu\text{g/L}$) and atrazine ($IC_{50} = 1.6 \mu\text{g/L}$). It is demonstrated that although R3 position of the haptin was employed to link to proteins and was considered to be less exposed to antibody recognition, the R3 group could provide hydrophobic force to the antigens, thus significantly increasing the antibody recognition. This conclusion coincided with our previous inference of antibody recognition of phenylurea herbicides (PUHs), which also have substituents at the same position as the one used to link to carrier proteins, providing hydrophobic forces to the PUH antigens.¹⁰ Therefore, it is further demonstrated that the hydrophobic contribution played by these less exposed protein-linking groups should not be ignored.

Three-Dimensional QSAR Analysis. Three-dimensional QSAR is applied to calculate the force field at 3D level. Steric fields, electrostatic fields, and other related descriptors are concerned in the calculations of 3D-QSAR. Three-dimensional QSAR analysis has been introduced to the antigen–antibody interaction study via the algorithm of comparative molecular field analysis (CoMFA).^{9,11} The standard CoMFA procedure requires the specification of both conformations and alignments of molecules. Meanwhile, only steric and electrostatic contributions are shown with the CoMFA model, but the hydrophobic contribution, which is generally considered as a critical force in antigen–antibody interaction, is not provided.⁸ Therefore, important information could be lost if CoMFA is used to explain antibody recognition. As an upgraded and complementary technique, comparative molecular similarity indices analysis (CoMSIA), introduces hydrophobic and hydrogen-bond indices to supplement the steric and electrostatic indices. Further, CoMSIA can reduce computational sensitivity to small changes in molecular alignments or grid orientations. The evaluation of CoMSIA fields is performed via a probe atom within lattice box, in which aligned molecules are embedded.^{28,29}

In the present study, CoMSIA QSAR model was employed to examine molecular effects on antibody recognition. Three physicochemical properties—steric, electrostatic, and hydro-

phobic fields—were evaluated to build the CoMSIA algorithm-based 3D-QSAR model. The CoMSIA analysis yielded R^2 of 0.997 with standard error of the estimate of 0.077, and the cross-validated correlation coefficient q^2 was 0.518. These statistical parameters validated acceptable correlation and predictability of the established model.

Contributions to antibody recognition of hydrophobic, steric, and electrostatic fields were 50.4%, 32.4%, and 17.2%, respectively. It was indicated that the hydrophobic interaction was the critical point of the triazine–antibody reaction, which coincided with correlation analysis described above. Steric and electrostatic variation also affected the antibody recognition significantly. The result of CoMSIA analysis was displayed as color-coded contours around the molecules, allowing visual identification of regions responsible for favorable/unfavorable interactions with the antibody (Figure 4).

For the hydrophobic interactions of R1 (Figure 4a), the graphic model indicates that the chlorine, sulfur, and oxygen atoms in R1 position had positive contributions to the hydrophobic interaction, so as to increase antibody recognition. However, the substituents linked to these atoms at R1 position led to decreased interaction by the hydrophobic fields. According to the steric model (Figure 4b), these substituents also sterically hindered the antibody recognition, which was generated by the hapten with only a chlorine atom in its R1 position. In the electrostatic model (Figure 4c), the chlorine, sulfur, and oxygen atoms in R1 position contributed positively to the reaction.

The substituents at R2 position approach R1 groups and have negative effects on the reaction, according to both hydrophobic and steric analyses (Figure 4a,b). Conversely, R2 groups with the same direction as that of the hapten provided positive steric contribution to the antibody recognition. The R3 substituents approaching R1, in the same direction as that of the hapten, provided hydrophobic and steric positive contributions to antibody recognition, while the dislocated ones had negative effects. This result coincided with HQSAR and indicated that not only did the dislocated direction of the substituents sterically hinder binding to the antibody but also the hydrophobicities misled the binding force.

On the basis of the CoMSIA model, it can be concluded that hydrophobic, steric, and electrostatic fields have played important roles in the antigen–antibody interaction. The chlorine, sulfur, and oxygen atoms in R1 position have provided electrostatic effects on antibody recognition. Meanwhile, the direction of the substituents in R2 and R3 groups is shown to be very important to the reaction, too. Even though the analytes had the same substituent in one position, different substituents in other positions may lead to the variation of its direction and affect the antibody recognition.

Spike and Recovery Study. Drinking water sample (purified water) free from triazines (checked by HPLC) was collected from the local market. Recoveries of the 11 triazine herbicides in drinking water were determined by icELISA. The sample water was spiked with triazines in different concentrations (three concentrations for each triazine: 1, 10, and 50 $\mu\text{g}/\text{L}$ for atrazine and propazine; 10, 20, and 50 $\mu\text{g}/\text{L}$ for prometryn, prometon, ametryn, and terbuthylazine; 50, 100, and 200 $\mu\text{g}/\text{L}$ for simazine and desmetryn; and 100, 200, and 500 $\mu\text{g}/\text{L}$ for terbutometon, simetryn, and terbutryn; three replicates for each test). Afterward, 9.55 mg of “PBS-forming ingredient” (containing 8 mg of NaCl, 0.2 mg of KCl, 1.15 mg of Na_2HPO_4 , and 0.2 mg of KH_2PO_4), which was the first time

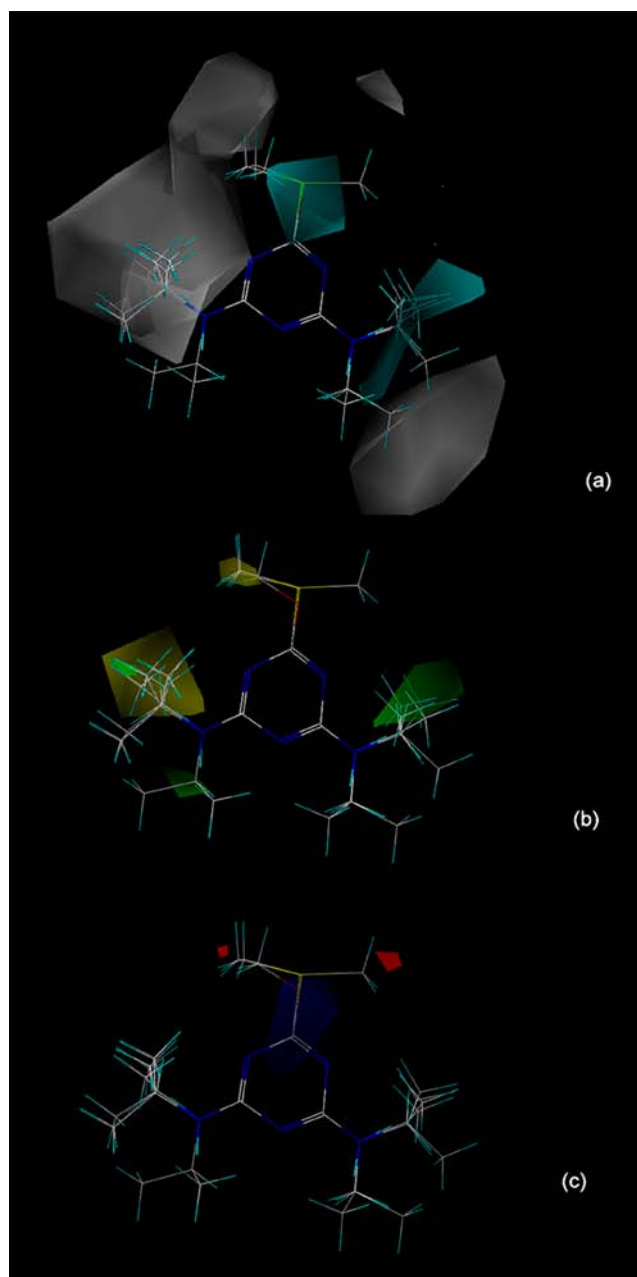


Figure 4. Contour bulks of CoMSIA hydrophobic, steric, and electrostatic fields. (a) Hydrophobic field: cyan contours indicate regions where groups increase antibody recognition (positive) and white contours indicate regions where groups decrease the activity (negative). (b) Steric field: green contours are for positive regions, yellow contours are for negative ones. (c) Electrostatic field: blue contours are for positive regions and red contours are for negative ones.

applied to eliminate the matrix effects as far as we know, was added to each milliliter of spiked water sample. Recoveries of the established ELISA for all triazine herbicides ranged from 72.2% to 116.8% (Figure 5). It was indicated that the “PBS-forming ingredient”, with which the PBS standard solution was imitated, could eliminate the matrix effect in purified water samples. This method provides not only convenient cleanup for accurate detection of water samples but also a pretreatment without any dilution step to remove matrix effects, which exponentially decrease the sensitivity. The immunoassay

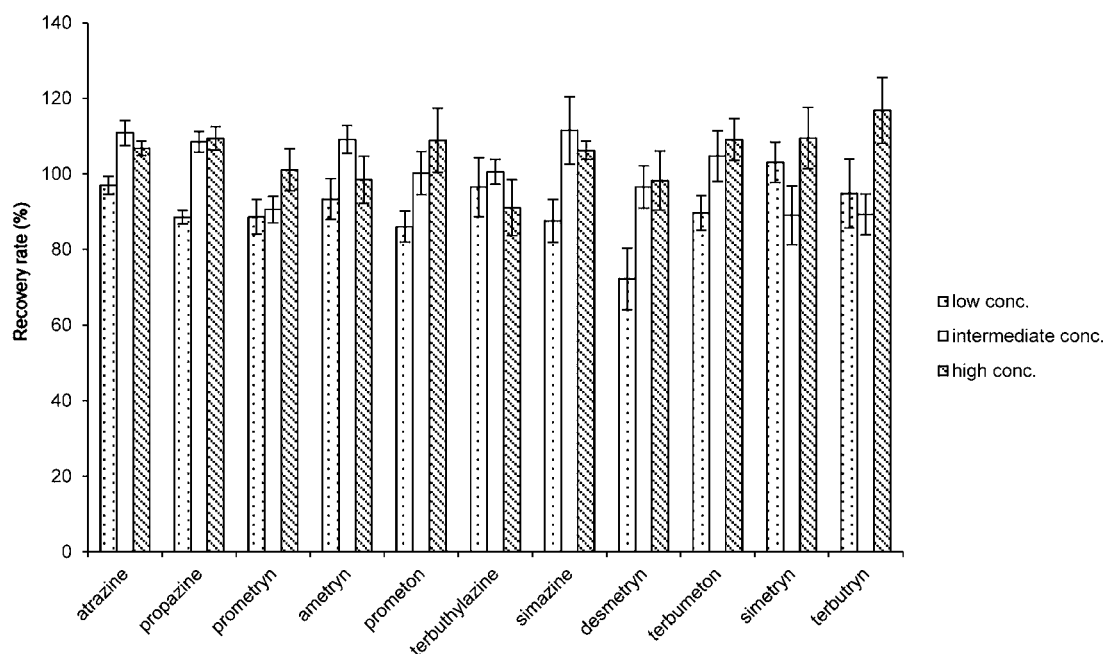


Figure 5. Recoveries of triazine herbicides in drinking water. Three concentrations were spiked for each triazine, and three replicates were performed for each test.

developed here can be suitable for the detection of trace levels of triazines in drinking water.

In the present study, a heterologous indirect competitive ELISA was established to detect 11 triazine herbicides with all LODs lower than 30 $\mu\text{g/L}$. To gain insight regarding the mechanism of antibody recognition, QSAR methodologies were applied to study the effects of different groups and properties of the analytes on the antigen–antibody interaction. The results demonstrated the following: (1) The antigens' hydrophobicity played the most important role in antibody recognition. (2) Hydrophobic, electrostatic, and steric properties of the analytes co-affected antibody recognition. (3) Frontier orbital energies and electrostatic fields of the R1 substituents affected antibody recognition. (4) Substituent groups of the analytes in dislocated directions caused steric hindrance and hydrophobic misleading of the antibody recognition, even though the antigens had the same substituents as the hapten. (5) A group of hapten used to link to carrier protein is less exposed to immune system and is consequently considered to be little contributive to the reaction.¹⁶ However, the substituents in this position could provide hydrophobic force to the antigens and thus significantly affect the antigen–antibody interaction.

Both GFA algorithm-based 2D-QSAR and CoMSIA algorithm-based 3D-QSAR were, for the first time, applied in the study of antigen–antibody interaction. This CAMM-based methodology was demonstrated as a suite of tools to provide insights into antibody recognition of small molecules.

■ ASSOCIATED CONTENT

📄 Supporting Information

One figure showing standard curves of triazine herbicide HeELISAs. This material is available free of charge via the Internet at <http://pubs.acs.org>.

■ AUTHOR INFORMATION

Corresponding Author

*Telephone (86 22) 60601456; fax (86 22) 60601332; e-mail s.wang@tust.edu.cn.

Notes

The authors declare no competing financial interest.

■ ACKNOWLEDGMENTS

We are grateful for financial support by the 973 project of the Chinese Ministry of Sciences and Technology (Project 2011CB512014), the National Natural Science Foundation of China (Project 31071547), and the Program for Changjiang Scholars and Innovative Research Team in University (Project IRT1166).

■ REFERENCES

- (1) Crowther, J. R. *The ELISA Guidebook*; Humana Press: Totowa, NJ, 2001; Vol. 149, pp 551.
- (2) Schneider, P.; Hammock, B. D. Influence of the ELISA format and the hapten–enzyme conjugate on the sensitivity of an immunoassay for s-triazine herbicides using monoclonal antibodies. *J. Agric. Food Chem.* **1992**, *40*, 525–530.
- (3) Goodrow, M. H.; Sanborn, J. R.; Stoutamire, D. W.; Gee, S. J.; Hammock, B. D. Strategies for immunoassay hapten design. *ACS Symp. Ser.* **1995**, *586*, 119–139.
- (4) Xu, Z. L.; Shen, Y. D.; Beier, R. C.; Yang, J. Y.; Lei, H. T.; Wang, H.; Sun, Y. M. Application of computer-assisted molecular modeling for immunoassay of low molecular weight food contaminants: A review. *Anal. Chim. Acta* **2009**, *647*, 125–136.
- (5) Wortberg, M.; Goodrow, M. H.; Gee, S. J.; Hammock, B. D. Immunoassay for simazine and atrazine with low cross-reactivity for propazine. *J. Agric. Food Chem.* **1996**, *44*, 2210–2219.
- (6) Delaunaybertoncini, N.; Pichon, V.; Hennion, M. Experimental comparison of three monoclonal antibodies for the class-selective immunoextraction of triazines: Correlation with molecular modeling and principal component analysis studies. *J. Chromatogr. A* **2003**, *999*, 3–15.
- (7) Beier, R. C.; Stanker, L. H. An antigen based on molecular modeling resulted in the development of a monoclonal antibody-based

immunoassay for the coccidiostat nicarbazin. *Anal. Chim. Acta* **2001**, *444*, 61–67.

(8) Xu, Z. L.; Wang, H.; Shen, Y. D.; Nichkova, M.; Lei, H. T.; Beier, R. C.; Zheng, W. X.; Yang, J. Y.; She, Z. G.; Sun, Y. M. Conformational changes of hapten-protein conjugates resulting in improved broad-specificity and sensitivity of an ELISA for organophosphorus pesticides. *Analyst* **2011**, *136*, 2512–2520.

(9) Wang, Z.; Zhu, Y.; Ding, S.; He, F.; Beier, R. C.; Li, J.; Jiang, H.; Feng, C.; Wan, Y.; Zhang, S.; Kai, Z.; Yang, X.; Shen, J. Development of a monoclonal antibody-based broad-specificity ELISA for fluoroquinolone antibiotics in foods and molecular modeling studies of cross-reactive compounds. *Anal. Chem.* **2007**, *79*, 4471–4483.

(10) Yuan, M.; Liu, B.; Liu, E.; Sheng, W.; Zhang, Y.; Crossan, A.; Kennedy, I.; Wang, S. Immunoassay for phenylurea herbicides: application of molecular modeling and quantitative structure–activity relationship analysis on an antigen–antibody interaction study. *Anal. Chem.* **2011**, *83*, 4767–4774.

(11) Xu, Z. L.; Shen, Y. D.; Zheng, W. X.; Beier, R. C.; Xie, G. M.; Dong, J. X.; Yang, J. Y.; Wang, H.; Lei, H. T.; She, Z. G.; Sun, Y. M. Broad-specificity immunoassay for *O,O*-diethyl organophosphorus pesticides: application of molecular modeling to improve assay sensitivity and study antibody recognition. *Anal. Chem.* **2010**, *82*, 9314–9321.

(12) Hayes, T. B.; Khoury, V.; Narayan, A.; Nazir, M.; Park, A.; Brown, T.; Adame, L.; Chan, E.; Buchholz, D.; Stueve, T. Atrazine induces complete feminization and chemical castration in male African clawed frogs (*Xenopus laevis*). *Proc. Natl. Acad. Sci. U.S.A.* **2010**, *107*, 4612.

(13) Na, Y.; Sheng, W.; Yuan, M.; Li, L.; Liu, B.; Zhang, Y.; Wang, S. Enzyme-linked immunosorbent assay and immunochromatographic strip for rapid detection of atrazine in water samples. *Microchim. Acta* **2012**, *177*, 177–184.

(14) Wang, S. T.; Gui, W. J.; Guo, Y. R.; Zhu, G. N. Preparation of a multi-hapten antigen and broad specificity polyclonal antibodies for a multiple pesticide immunoassay. *Anal. Chim. Acta* **2007**, *587*, 287–292.

(15) Wang, S.; Allan, R. D.; Skerritt, J. H.; Kennedy, I. R. Development of a class-specific competitive ELISA for the benzoylphenylurea insecticides. *J. Agric. Food Chem.* **1998**, *46*, 3330–3338.

(16) Duan, J.; Yuan, Z. Development of an indirect competitive ELISA for ciprofloxacin residues in food animal edible tissues. *J. Agric. Food Chem.* **2001**, *49*, 1087–1089.

(17) Van Coillie, E.; De Block, J.; Reybroeck, W. Development of an indirect competitive ELISA for flumequine residues in raw milk using chicken egg yolk antibodies. *J. Agric. Food Chem.* **2004**, *52*, 4975–4978.

(18) Hocquet, A.; Langgard, M. An evaluation of the MM+ force field. *J. Mol. Model.* **1998**, *4*, 94–112.

(19) Dewar, M. J. S.; Zoebisch, E. G.; Healy, E. F.; Stewart, J. J. P. Development and use of quantum mechanical molecular models. 76. AM1: a new general purpose quantum mechanical molecular model. *J. Am. Chem. Soc.* **1985**, *107*, 3902–3909.

(20) Harrison, R. O.; Goodrow, M. H.; Hammock, B. D. Competitive inhibition ELISA for the *s*-triazine herbicides: assay optimization and antibody characterization. *J. Agric. Food Chem.* **1991**, *39*, 122–128.

(21) Beier, R. C.; Ripley, L. H.; Young, C. R.; Kaiser, C. M. Production, characterization, and cross-reactivity studies of monoclonal antibodies against the coccidiostat nicarbazin. *J. Agric. Food Chem.* **2001**, *49*, 4542–4552.

(22) Lee, N.; Rachmawati, S. A rapid ELISA for screening aflatoxin B1 in animal feed and feed ingredients in Indonesia. *Food Agric. Immunol.* **2006**, *17*, 91–104.

(23) Devillers, J.; Balaban, A. T. *Topological Indices and Related Descriptors in QSAR and QSPR*; CRC Press: Boca Raton, FL, 1999; pp 1–2.

(24) Rogers, D.; Hopfinger, A. Application of genetic function approximation to quantitative structure–activity relationships and

quantitative structure–property relationships. *J. Chem. Inf. Model.* **1994**, *34*, 854–866.

(25) Lu, X.; Webb, M.; Talbott, M.; Van Eenennaam, J.; Palumbo, A.; Linares-Casenave, J.; Doroshov, S.; Struffenegger, P.; Rasco, B. Distinguishing ovarian maturity of farmed white sturgeon (*Acipenser transmontanus*) by Fourier transform infrared spectroscopy: a potential tool for caviar production management. *J. Agric. Food Chem.* **2010**, *58*, 4056–4064.

(26) Xu, Z. L.; Xie, G. M.; Li, Y. X.; Wang, B. F.; Beier, R. C.; Lei, H. T.; Wang, H.; Shen, Y. D.; Sun, Y. M. Production and characterization of a broad-specificity polyclonal antibody for *O,O*-diethyl organophosphorus pesticides and a quantitative structure–activity relationship study of antibody recognition. *Anal. Chim. Acta* **2009**, *647*, 90–96.

(27) Heritage, T. W.; Lewis, D. R. *Molecular Hologram QSAR*. In *Rational Drug Design*; ACS Symposium Series, Vol. 719; American Chemical Society: Washington DC, 1999; pp 212–225.

(28) Klebe, G.; Abraham, U.; Mietzner, T. Molecular similarity indices in a comparative analysis (CoMSIA) of drug molecules to correlate and predict their biological activity. *J. Med. Chem.* **1994**, *37*, 4130–4146.

(29) Klebe, G.; Abraham, U. Comparative molecular similarity index analysis (CoMSIA) to study hydrogen-bonding properties and to score combinatorial libraries. *J. Comput.-Aided Mol. Des.* **1999**, *13*, 1–10.